

TWO-WAY SPANNING CLT-CONCRETE-COMPOSITE-SLABS

S. Loebus, P. Dietsch & S. Winter

Chairs of Timber Structures and Building Construction, TUM

This paper was originally published for the 2017 INTER Conference.

KEYWORDS

Timber-concrete-composite, cross-laminated timber, two-way spanning slab, shear connection, notch, fully threaded screw, plate load-bearing behaviour, force-fitting element joint.

1 INTRODUCTION

This contribution deals with investigations on the load-bearing behaviour of two-way spanning cross-laminated-timber-concrete-composite slabs (CLTCC). To this aim, different examinations on shear connectors, slabs and slab sections, as well as on force-fitting element joints were realized. The examination contains experimental tests of different scale, FEM-simulations and static spring-models.

Cross-laminated timber (CLT) was selected for the timber layer, as it is capable of bearing load biaxially. Two shear connectors, for which the load bearing behaviour in uniaxial timber-concrete-composite (TCC) systems is well known, were examined in a two-way spanning system: Fully threaded screws applied at an angle of 45° to the grain and rectangular notches. For both connections adequate construction guidelines in the given biaxial stress field and in combination with cross-laminated-timber will be

presented.

As transportation and production limit the element size of cross-laminated timber, a force-fitting element joint is necessary to activate the biaxial load-bearing capacity. With glued-in reinforcement bars, a connection will be shown, which meets both requirements of stiffness and practical buildability.

Prior to the investigations, the following boundary conditions were specified, see Table 1.

In addition, the effect of torsion and the interaction of the principal span directions in x- and y- axis are examined.

For a better understanding of the plate load-bearing behaviour, the slab is examined in real tests and a solid FE-model with individual layer and connection detailing. Simplified solutions for a continuous and homogenous distributed shear stiffness and a representation of the element joint are given and are meant as the foundation for a further simplified plate

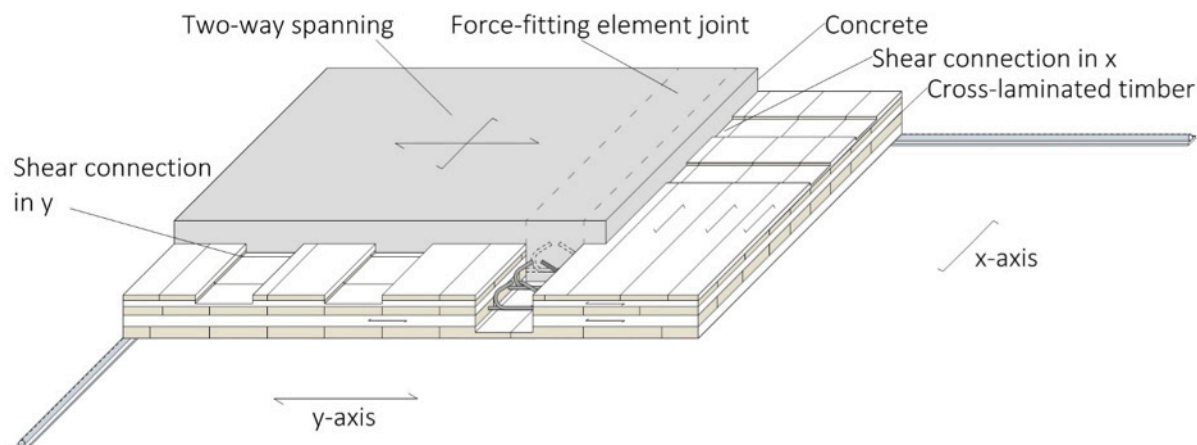


Figure 1: Two-way spanning cross-laminated-timber-concrete-composite slab.

Table 1. Overview of parameters and boundary conditions.

Parameter	Value
Concrete	Strength class C20/25; very pourable (>F5); min. reinforcement $A_{min} = 1.88 \text{ cm}^2/\text{m}$ in each direction; Layer thickness $t_{concrete} = 60 - 80 \text{ mm}$
Cross-laminated timber	Strength class C24; Individual Layer thickness $t_{layer} = 20 / 30 / 40 \text{ mm}$; Maximum 5 layers; $t_{CLT} = 120 - 160 \text{ mm}$
Shear connection	Notch - rectangular, not reinforced; in different sizes; Fully-threaded screw with 45° to the grain, $d = 8.0 \text{ mm}$, $l = 160 \text{ mm}$, $l_{ef,timber} = 110 \text{ mm}$
Separation layer between concrete and timber	None
Supports	All-side hinged; No hold against lifting
Side length ratio	$L_y / L_x = 1$
Element joint	Glued-in reinforcement bars

model.

Within the FEM simulations, the given two-spanning system is compared to common one-way spanning timber-concrete-composite systems.

It was attempted to describe the most important aspects of the research results to the given topic. Due to the length of this paper, some simplifications in the description had to be made. For detailed information, see [Loebus, 2017].

2 SHEAR CONNECTION

2.1 Alignment in plane

The load bearing behaviour of the given shear connectors, fully threaded screws applied at an angle of 45° to the grain and rectangular notches, is well known for uniaxial timber-concrete-composite systems, e.g. [Blaß et al., 1995] and [Michelfelder, 2006]. In the following, the connectors are examined in a two-way spanning system. In a stress field of a plate, the alignment of the connectors in plane becomes relevant. The connector follows either the alignment of principal stress or the given orthogonal alignment of the CLT. In fabrication, the notch

cutting procedure fits an orthogonal alignment and an alignment to wood grain direction, while the screw can be placed freely in plane without a bigger effort and is independent from the grain direction, when neglecting the embedment. Therefore, the screw can be aligned along the direction of principal shear forces. The alignment of shear connections is schematically shown in Figure 2.

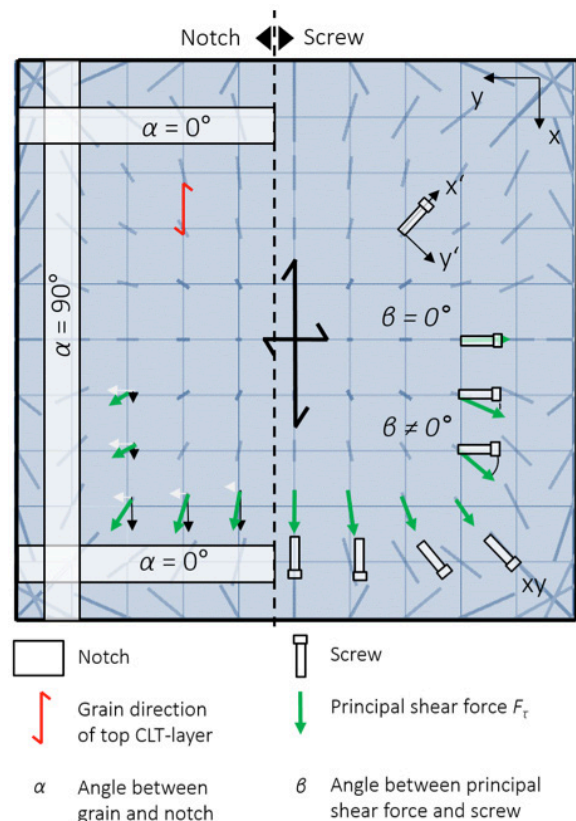


Figure 2: Alignment of shear connection in plane (for plane definition compare also Figure 6).

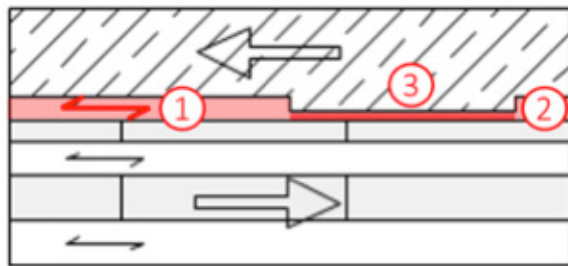
2.2 Notch

2.2.1 General

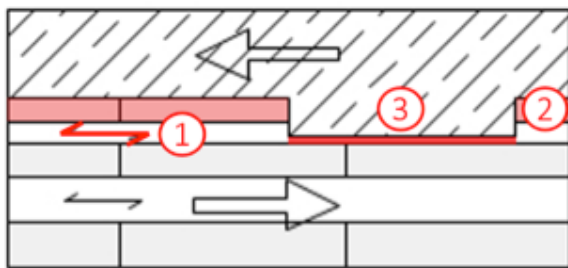
The load-bearing behaviour of notches in a one-way spanning system and in solid wood was recently summarized in [Kudla, 2015]. The slip modulus K_{ser} varies between 800 to 1,800 kN/mm/m, the load bearing capacity F_u between 520 and 730 kN/m. Regarding the two-way spanning CLT-concrete-composite system, two issues have to be dealt with: (1) The rolling shear perpendicular to grain in the CLT as an additional semi-rigidity in the cross-section in both load-bearing axis. (2) The obligatory activation of the y-axis (see Figure 1) with an effective smaller static height than the x-axis.

To develop a notch connection that works in both axis of the CLT, FEM-simulations, two-sided push out

tests and parametric studies were performed. The derived construction guidelines and load-bearing characteristics are given in the following. Three major issues were identified, given in Figure 3.



a) Notch parallel to grain ($a = 0^\circ$)



b) Notch perpendicular to grain ($a = 90^\circ$)

Figure 3: Notch construction overview with (1) Load application into timber (2) Top layer thickness (3) Activating a larger area for transmitting shear stress into the next layer by hanging back the timber in front of the notch below the notch.

2.2.2 Shear load application into CLT

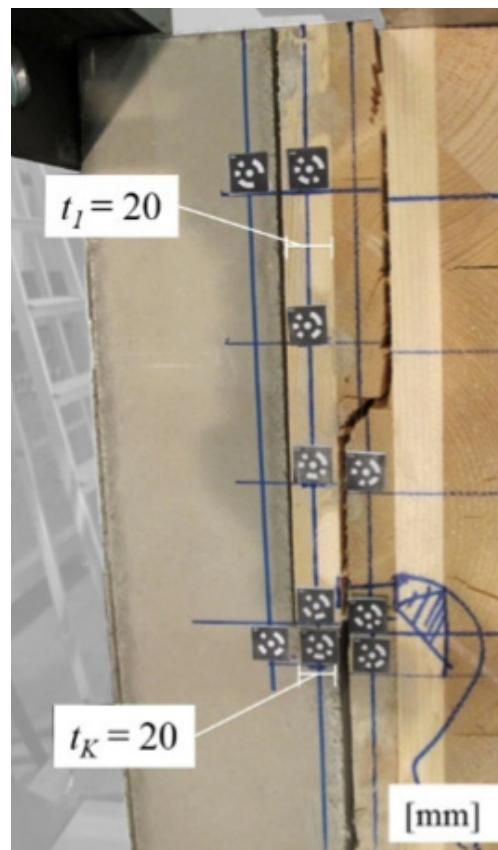
The evaluation of the push-out shear test as shown in Figure 4 and Table 2 show, that a notch connection perpendicular to grain reaches only a fraction of load-bearing capacity and shear stiffness compared to a notch parallel to grain. Even if there is barrier effect of the next CLT-layer, the notch design in y-axis cannot be the same as in x-axis. To activate both axis equally from the perspective of shear stiffness, it is necessary to ensure a load application parallel to grain in both axis, as shown in Figure 3 no. 1.

2.2.3 Influence of the top CLT-layers

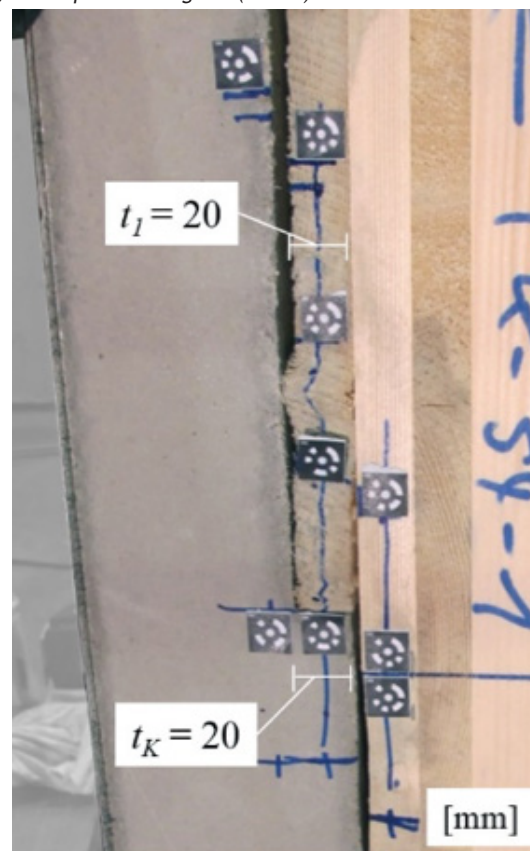
In consequence of the necessity to apply the shear load parallel to grain in each plate axis and respecting the fact that with increasing total notch depth the size of tension stress in the concrete console increases, the top layers should be kept relatively thin, see Figure 3 no. 2. As the element-joint requires a certain thickness in the bottom CLT-layers, later shown in Section 3, this leads to an asymmetric CLT-layer setup.

2.2.4 Depth of notch in load-bearing CLT-layer

Regarding the characteristics of a notch in CLT, the dominant parameter is the rolling shear stiffness



a) Notch parallel to grain ($a = 0^\circ$)



b) Notch perpendicular to grain ($a = 90^\circ$)

Figure 4: Failure mechanisms from push-out tests - Material according to Table 1. Notch depth $t_k = 20$ mm; Top and second CLT-layer $t_1 = t_2 = 20$ mm; Notch length $l_n = 200$ mm; Timber length in front of the notch $l_v = 250$ mm.

Table 2. Test results: Push-out tests according to Figure 4 and [EN 26891].

α	$t_{concrete}^*$	$F_{u,mean}$	F_k	CV(F)	$k_{s,mean}$	CV(k_s)	N
[°]	[days]	[kN/m]	[kN/m]	[%]	[kN/mm/m]	[%]	[Piece]
0	17	344.7	295.9	6.5	676.5	30.1	3
0	120	370.5	322.0	1.6	759.5	25.3	2
90	17	97.4	86.5	3.5	134.0	15.6	3
90	120	124.7	106.5	4.8	83.1	5.1	2

* The first series was tested after reaching the minimum concrete strength C20/25 after $t_{concrete} = 17$ days. The top CLT-layer had relatively high humidity (~25%). After $t_{concrete} = 120$ days a second series was tested with reduced humidity.

of CLT-layers perpendicular to grain, as seen in the failure pictures of Figure 4. The transfer of shear stress from the notch to the next soft shear layer can be improved by enlarging the effective contact length between both layers. Therefore, to enlarge the shear transmission area between the layers, the timber in front of the notch should be hanged back beneath the notch, see Figure 3 no. 3 and the comparison in Figure 5. In addition, gaps in CLT without edgewise bonding are bypassed more effectively, if the transmission area is larger.

2.3 Screw

2.3.1 General

The load-bearing behaviour of screwed shear connections is examined exemplarily with the fully-thread screw ASSY Plus, because it has a German and a European Technical Approval, [Z-9.1-648] and [ETA-13/0029], for CLT-concrete-composites. The slip moduli in those approvals differ. Therefore, they are both taken into consideration. The examinations on the biaxial load-bearing behaviour can be transferred to other screw-types as long as the according slip moduli are given.

2.3.2 Differentiation in axial and lateral load application

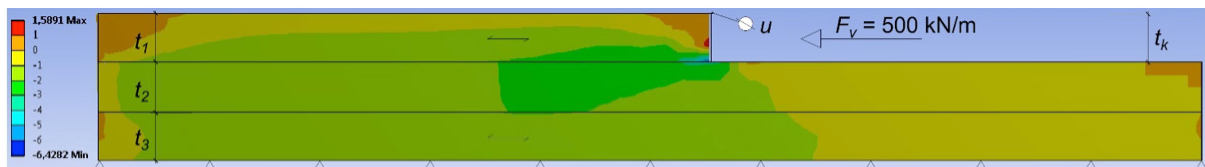
From the perspective of the screw, it is differentiated

between axial (x') and lateral (y') load application in plane, see Figure 6. Both load directions feature an individual load bearing capacity and slip modulus, see Table 3.

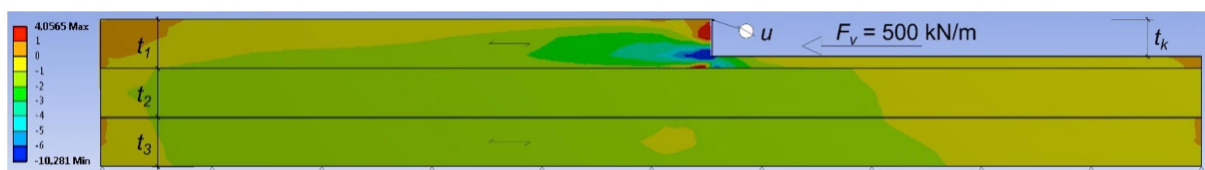
According to Figure 7, the principal shear force F can be distributed on the equivalent slip moduli K_{ax} and K_{lat} , represented as vectorised springs. From the resulting slip u_{ax} and u_{lat} the total slip u_{tot} and together with F , the total slip modulus K_{tot} can be derived. In practice the application of K_{tot} as relevant slip modulus is difficult in use, because the spring vector of K_{tot} is not in direction of $F(B)$. For $0^\circ < \beta < 90^\circ$ the orthotropic slip moduli lead to a deviating slip $u_{|F}$ perpendicular to the force F . As the screws are applied in a bundle, it is assumed that the potential slip $u_{|F}$ is braced by a force redistribution on surrounding screws in other directions. Consequently, $K_{||F}$ is used as relevant slip modulus.

The slip modulus in direction of the principal shear force $K_{||F}$ can be calculated according to Equation 1:

$$K_{||F} = \left[\frac{\cos^2 \beta}{K_{ax}} + \frac{\sin^2 \beta}{K_{lat}} \right]^{-1} \quad (1)$$

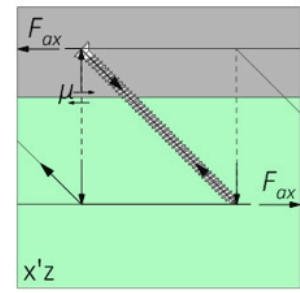
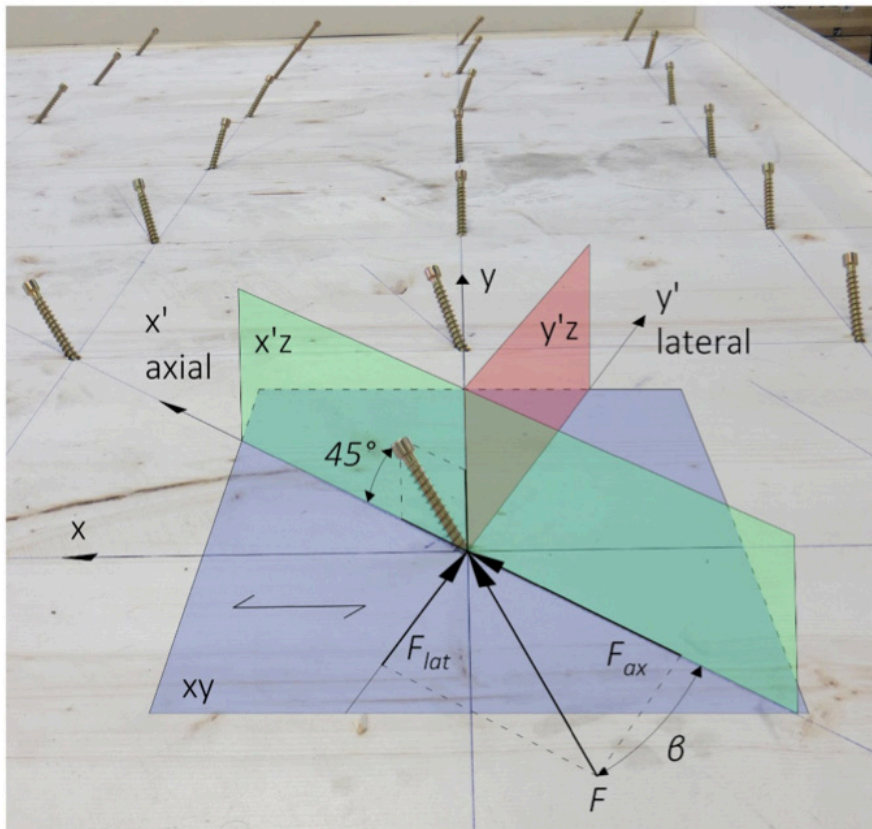


a) Notch depth $t_k = 20$ mm, without hanger for timber in front of the notch; $K_{ser} = F_v / u = 584$ kN/mm/m

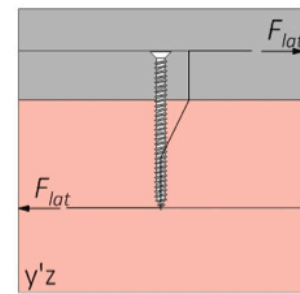


b) Notch depth $t_k = 15$ mm, hanger thickness $\Delta t = t_1 - t_k = 5$ mm beneath the notch; $K_{ser} = 707$ kN/mm/m

Figure 5: Comparing the effect of a hanger for the timber in front of the notch by a shear stress distribution τ_{xz} [N/mm²] with CLT-layer thickness $t_1 = t_2 = t_3 = 20$ mm [ANSYS 17.1].



b) Axial (ax)



c) Lateral (lat)

a) Photo of the screw connection and the CLT of a plate test specimen, described in detail in Section 4. For an exemplary screw plane, sections, and force distribution are visualised.

Figure 6: Load application on a screw shear connection. Dimensions according to Table 1.

Table 3. Load-bearing capacity and slip modulus of a fully-threaded screw timber-concrete-composite connection with screws according to [ETA-13/0029] and [Z-9.1.-648]; $\rho_k = 350 \text{ kg/m}^3$

	Axial ($\beta = 0^\circ$)		Lateral ($\beta = 90^\circ$)		Ratio axial / lateral			
	ETA ($\mu^* = 0.25/0$)	abZ	ETA	abZ	ETA ($\mu = 0.25/0$)	abZ		
F_{Rk}	7.8 / 6.2	6.2	3.1	3.6	[kN]	2.5 / 2.0	1.7	[-]
K_{ser}	11.0	11.0	2.0	1.5	[kN/mm]	5.5	7.3	[-]

* μ = friction coefficient concrete-timber

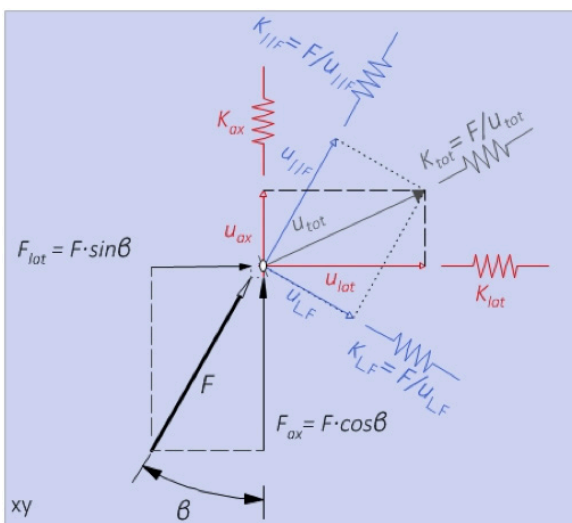


Figure 7: Slip behaviour due to an orthotropic slip modulus (K_{ax} ; K_{lat}).

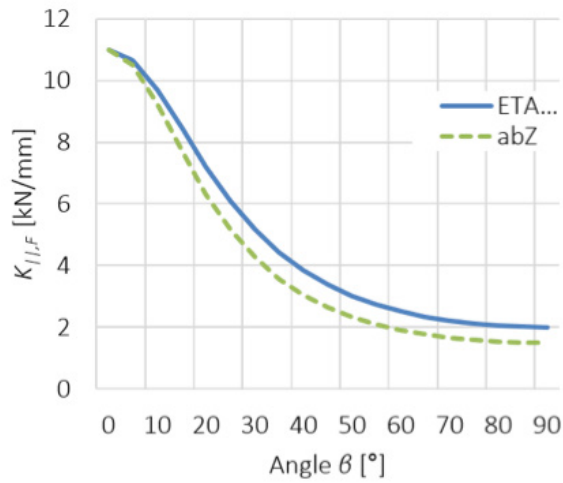
Combining the load-bearing capacity according to [DIN EN 1995-1-1] Equation 8.28 the maximum value depending on the angle β according to Figure 6 and Figure 7 is given in Equation 2:

$$F_{Rd} = \left[\left(\frac{\cos \beta}{F_{Rd,ax}} \right)^2 + \left(\frac{\sin \beta}{F_{Rd,lat}} \right)^2 \right]^{-0.5} \quad (2)$$

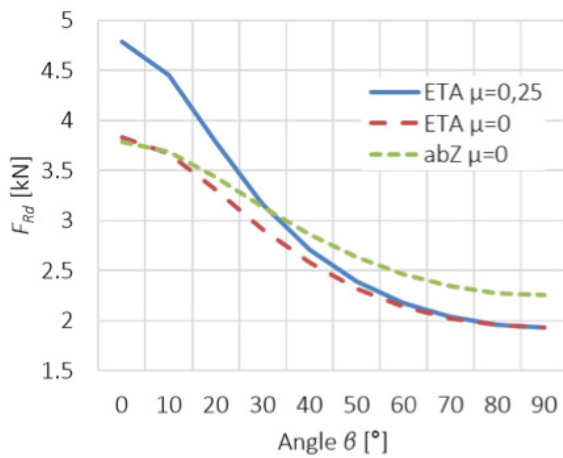
A distribution of $K_{1|F}$ and F_{Rd} is given in Figure 8. It shows a logarithmic reduction in dependence on β .

The load-bearing behaviour of the connection under a deviating angle of application β was subject to push-out shear tests, Figure 9. Results and testing parameter are summarized in Table 4.

While the absolute values of the results deviate, the ratio $\beta / 0^\circ$ for $t_{concrete} = 120$ days shows good agreement with the slip moduli from the technical approvals, see Table 5.



a) Slip modulus $K_{||F}$



b) Load-bearing capacity F_{Rd}

Figure 8: Slip modulus and load-bearing capacity in dependence on β for a shear connection with screws according to Table 3.

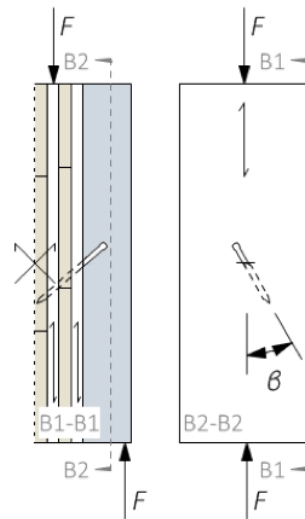


Figure 9: Testing scheme push-out test fully-threaded screw.

A direction change of the force F due to the orthotropic slip modulus is neglected under the assumption that the screw is aligned to the principal shear force as close as possible. By aligning the screw to the principal shear force in plane, an isotropic slip modulus K_A may be assumed in plane of the shear connection. A deviating force application angle can occur however, if load situations, long-term behaviour or discretization in the screw alignment change, and therefore should be taken into account by applying $K_{||F}(\beta_{deviate})$, according to Equation 1 or Figure 8a.

Table 4. Test results: Push-out test on timber-concrete-composite connections with fully-threaded screw according to Table 1, Table 3, Figure 9 and [EN 26891].

β [°]	$t_{concrete}^*$ [days]	$F_{u,mean}$ [kN/m]	F_k [kN/m]	CV(F) [%]	$k_{s,mean}$ [kN/mm/m]	CV(k_s) [%]	N [Piece]
0	17	21.1	18.7	2.0	80.3	15.5	3
0	120	21.8	15.3	10.8	41.9	7.2	2
30	17	19.1	17.0	4.6	54.8	30.3	3
30	120	20.1	17.4	1.9	18.9	17.7	2
60	17	14.7	11.7	9.2	47.1	38.6	3
60	120	15.4	13.4	1.4	7.1	16.4	2

* The first series was tested after reaching the minimum concrete strength C20/25 after $t_{concrete}=17$ days. The top CLT-layer had relatively high humidity (~25%). After $t_{concrete} = 120$ days a second series was tested with reduced humidity.

Table 5. Comparison of the slip moduli from the approvals (ETA/abZ) and the push-out test results ($t_{concrete} = 17d / 120d$) in dependence on β .

β [°]	$K_{ F}$ [kN/mm]		$K_{ F,\beta} / K_{ F,0^\circ}$ [-]		$k_{s,mean}$ [kN/mm]		$k_{s,\beta} / k_{s,0^\circ}$ [-]	
	ETA	abZ	ETA	abZ	17d	120d	17d	120d
0	11.0	11.0	1.00	1.00	80.3	41.9	1.00	1.00
30	5.2	4.3	0.47	0.39	54.8	18.9	0.68	0.45
60	2.5	1.9	0.23	0.17	47.1	7.1	0.59	0.17

3 FORCE-FITTING ELEMENT JOINT

As transportation and production limit the CLT-element size, a force-fitting element joint is necessary to activate the biaxial load-bearing capacity. Most important parameter is the effective bending stiffness of the joint connection. A reduction in stiffness reduces the stiffness of the respective axis orthogonal to the joint and therefore a balanced biaxial load-bearing behaviour. As the concrete layer can be realized in one piece, the focus lies on the element joint between the CLT-elements, in particular the lowest CLT-layer with the resulting tension force Z parallel to grain, compare Figure 10a.

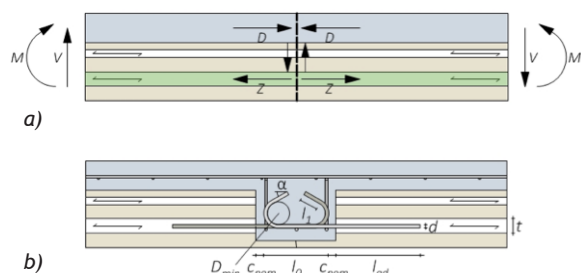


Figure 10: Force-fitting element joint - a) forces to be transferred and b) joint connection with glued-in reinforcement bars.

Different connection types, such as fully threaded screws applied crosswise under 45° and 135° or gluing, were compared. With glued-in reinforcement bars, Figure 1 and Figure 10b, a connection was developed, which meets the requirements of stiffness and practical buildability.

Glued-in steel bars are a very stiff connection-type in timber engineering. If reinforcement bars are used as steel bars, the connection can be applied in concrete as well. In the concrete, the bars of two CLT-elements can be overlapped and jointed force-fittingly. The bars are curved to reduce the overlapping length.

The concrete-part of the connection can be designed according to [EN 1992-1-1] Sec. 8. For the timber-part, information can be found in [Steiger, 2012] and

requirements according to [DIN EN 1995-1-1/NA 11.2].

To minimise the loss in stiffness, the stiffness of the steel bars EA_{steel} should be equal to the stiffness of the corresponding CLT-layer (in green in Figure 10a) EA_{timber} . From the perspective of minimum spacing, this requirement complies with a layer thickness of 30 mm as shown in the results of a parametric study, see Table 6.

The performance of the connection was verified in a four-point bending test as shown in Figure 11. In addition to the specimen featuring the element-joint, reference specimens with a continuous CLT-element were tested. The connection was realised with nine reinforcement bars per metre, $d = 10.0$ mm, on each element side, which resembles 45% of the jointed timber layer stiffness. The reason to stay below the full stiffness of the timber layer was to provoke a ductile failure in the steel bars and to keep the connection in an economical format. Further specimen specifications are given in Table 8.

The test results show a similar deflection behaviour of the jointed elements in comparison to those without. The overall loss in stiffness is smaller than expected. The low stiffness of the effective steel cross section in comparison to the jointed timber layer is compensated by a stiffening effect of the concrete block. Further, the failure behaviour is ductile, because of the yielding of the steel bars. The elements can be joined with barely any loss in stiffness and failure load can be determined more precisely, compare Table 7.

4 PLATE LOAD-BEARING BEHAVIOUR

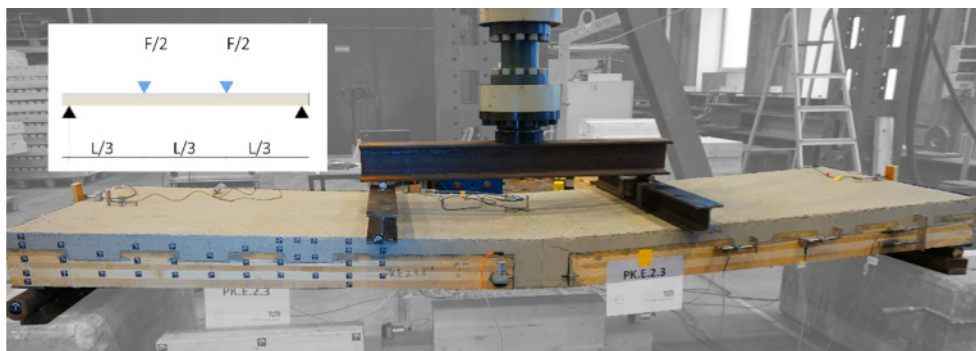
4.1 General

The plate load-bearing behaviour was examined in two plate test series and accompanying FEM-simulations. The tests included a torsion test on a plate section and full plate tests in analogy to a uniaxial four-point-

Table 6. Parametric study of the connection 'steel bars glued in CLT-layer'.

Geometry		Aim: $EA_{steel} / EA_{timber} = 1.0$		Limit: $a_{z,req} = 5d$ & $a_{z,c,req} = 2.5d$	
$t_{CLT-layer}$ [mm]	d_{bar} [mm]	n_{bar} [Piece/m]	a_z [mm]	$n_{bar,max}$ [Piece/m]	max EA_{steel} / EA_{timber}
30	8	31	32	4d	0.8
30	10	20	50	5d	1.0
30	12	14	72	6d	1.2
40	8	42	24	3d	0.6
40	10	27	37	3.7d	0.75
40	12	19	54	4.5d	0.9

With $E_{timber} = 11,000 \text{ N/mm}^2$, $E_{steel} = 210,000 \text{ N/mm}^2$, according to [DIN EN 1995-1-1/NA] Tab. NA.22



a) Four-point bending test scheme and test setup with $L=3.4$ m. In this picture the element-joint fails.



b) Steel bar failure

Figure 11: Test on one-way spanning slab, 3.5 m \times 1.0 m, with a force-fitting element joint analogous to the section in y -axis in Figure 1.

Table 7. Test results of the four-point bending test. For comparative reasons equivalent stiffness moduli k_s and k_u were calculated based on [EN 26891].

Element joint	$F_{u,mean}$	$CV(F_u)$	$k_{s,mean}$	$CV(k_s)$	$k_{u,mean}$	$CV(k_u)$	N
	[kN]	[%]	[kN/mm/m]	[%]	[kN/mm/m]	[%]	[Piece]
No	113.05	15.6	3.98	2.7	3.09	16.5	3
Yes	90.40	3.0	3.87	9.1	2.14	19.2	3
Ratio	$F_{u,mean}$		$k_{s,mean}$		$k_{u,mean}$		
Yes / No [%]	80.0		97.2		69.3		

bending test, Figure 12a. Apart from the individual failure mechanism and the maximum load-bearing capacity, the stiffness of the plate and potential improvement of the serviceability in comparison to existing one-way-spanning timber-concrete-composite slabs were objects of interest.

4.2 Experimental behaviour

The specimens match in the application of the shear connectors according to the proposed alignment in Section 2: Notches in an orthogonal alignment and screws following the direction of principal shear force in the plane of the slab, Figure 12b, c. Specimen parameters are given in Table 8. The results show a high load-bearing capacity and a constant deformation behaviour along a long range of the load level. The failure mechanism is successive and ductile. The specimens show a similar high level of stiffness up to

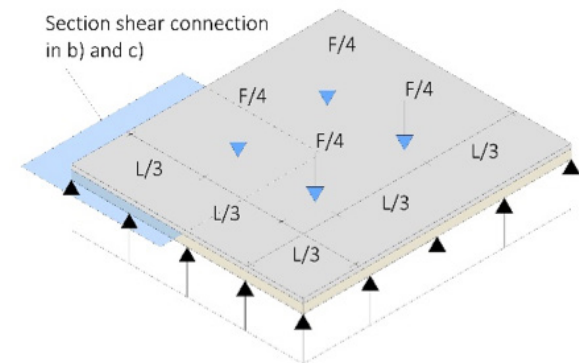
Table 8. Specimen parameters to the plate and element joint tests.

Layer thickness		Screw		trajectorially aligned	
Concrete	60 mm	Total length l - diameter d	160 mm - 8.0 mm		
CLT	20-20 20-30 30 mm	Effective length $l_{ef,timber}$	110 mm		
Shear Connection		Angle in cross-section	45°		
Notch ($\alpha = 0^\circ$)	orthogonally aligned	Distances $a_x \times a_y$	250 mm \times 250 mm		
Length $l_N \times$ Depth t_N	140 mm \times 15 mm	Discretisation angle in plane	22.5°		
Length in front of notch l_v	200 mm	Slab lengths			
Notch ($\alpha = 90^\circ$)	orthogonally aligned	Total	3,500 mm		
Length $l_N \times$ Depth t_N	160 mm \times 35 mm	Support width	100 mm		
Length in front of notch l_v	180 mm	Span L	3,400 mm		

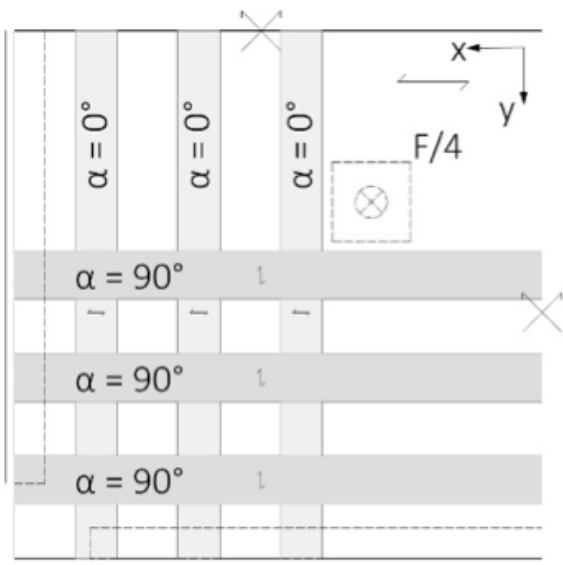
a load of approximately 55 % F_u , independent from the shear connector, Figure 13. Both systems reached a similar level of maximum load, which is characterized by the final failure of the lowest layer of the CLT. This was preceded by a failure of the concrete layer.

4.3 FEM-Model

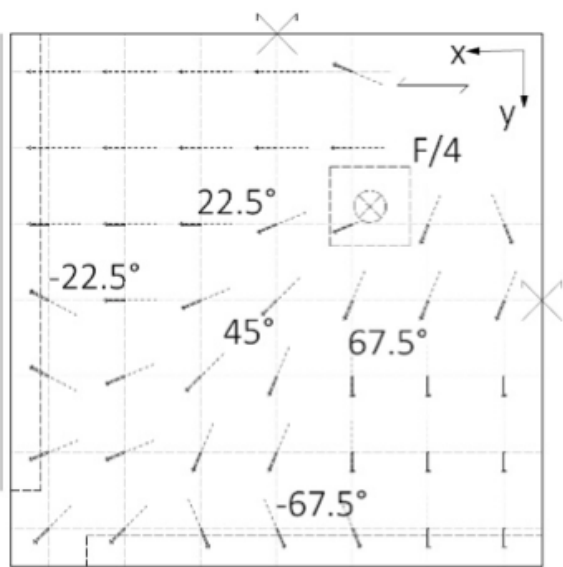
The experimental examinations were accompanied by FEM-simulations. The slab with notches as shear connectors was simulated in a fully scaled solid model. For the screws a simplified model was developed. In the simplified model, the shear stiffness of the screw connection is distributed uniformly over the plane of the slab and is transferred into the top CLT-layer by calculating the slip modulus of the screws into the shear modulus. With this method, the modelling and processing effort was reduced a lot. Potential shear reinforcement effects of the inclined screws on the



a) Test setup



b) Notch shear connection



c) Screw shear connection

Figure 12: Full plate test - Setup and specific specimen design.

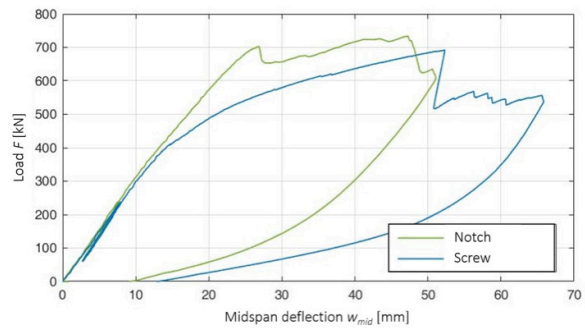


Figure 13: Load-deflection-curve to full plate test.

CLT-element are not covered. In comparison, the FEM-models behave softer than the plate test results. From the perspective of serviceability, this behaviour is on the safe side. The simplified model is applied on investigations in the next Sections 4.4 - 4.7.

4.4 Biaxial load-bearing behaviour

In the FEM-simulation following the full plate test setup, the effective biaxial load-bearing behaviour of the composite-slab was evaluated by comparing the vertical support reactions in principal and transverse direction. In a perfect isotropic plate, a uniformly distributed load would spread 50/50 into the supports of both axis. For the orthotropic CLT-concrete-composite-slab, the load distributes in a range of 55/45 to 58/42. This demonstrates a clear biaxial load-bearing behaviour.

4.5 Torsion

The torsional bending is an essential mechanism of the load bearing behaviour of a plate. In experimental examinations regarding the torsional bending stiffness, the influence of different construction parameters such as CLT-layer configuration or shear connectors was quantified. The composite-slab behaves very ductile when exposed to torsional bending, the ultimate force was not reached while the deflection exceeded the testing setup limits with $w_{max} > L/30$. The cracking of the concrete layer results in a considerable loss of torsional bending stiffness. The samples with $h_{concrete}/h_{CLT} = 0.5$ and $L/h = 8.5$ showed a loss of 58% - 67%. The minimum reinforcement was not taken into account, as it was placed in middle height of the concrete layer. To quantify the share and the influence of the torsional behaviour on the plate load-bearing behaviour, the shear modulus in plane was compared for all materials in the FEM-simulation ($G_{xy,FEM} = G_{xy,material}$ vs. $G_{xy,FEM} = 0$). As a result, the deflection of a two-way spanning composite slab with torsional stiffness close to zero is about 25% higher in

comparison to a slab with uncracked concrete (with $L/h = 19$).

4.6 Comparison

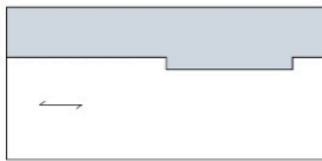
Based on the earlier investigations, FEM-simulations on different slab assemblies in one-way and two-way spanning directions and side lengths $L_x \times L_y = 6.0$ m were conducted, see Figure 14. Material properties accord with Table 1. For the shear connection a continuous distributed slip modulus in plane $K_A = 1,778$ kN/mm/m² was taken, which equates to a notch connection with $K_{ser} = 800$ kN/mm/m every 0.45 m. The applied element joint stiffness with $EA_{steel} =$

$0.54 \cdot EA_{CLT-layer}$ results from ten reinforcement bars per metre and side with $d = 12.0$ mm. The full load value was set to $p_{k,inst} = 7.9$ kN/m² and $p_{k,q-p} = 6.7$ kN/m². The benchmark of comparison was the serviceability limit state with the characteristic midspan deflection w_{inst} and final deflection w_{fin} . Having the same height, the deflection w_{inst} reduces by 38.8% from one-way spanning CLTCC to two-way CLTCC + joint and by 14.3% from one-way TCC to two-way CLTCC + joint.

4.7 Side length ratio

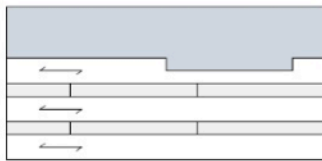
The influence of the side length ratio on the characteristic deflection w_{inst} was determined by FEM

One-way spanning TCC



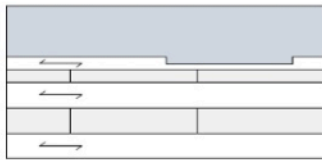
x
Concrete 80 Timber 160

One-way spanning CLTCC

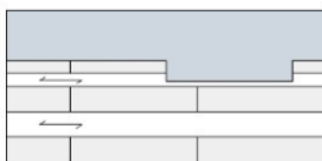


x
Concrete 80 CLT 160 (|40-20|40-20|40)

Two-way spanning CLTCC



x
Concrete 80 CLT 160 (|20-20|40-40|40)



y
Concrete 80 CLT 160 (-20|20-40|40-40)

Element joint for two-way spanning CLTCC



y
Element joint stiffness $EA_{steel} = 0.54 \cdot EA_{CLT-layer}$

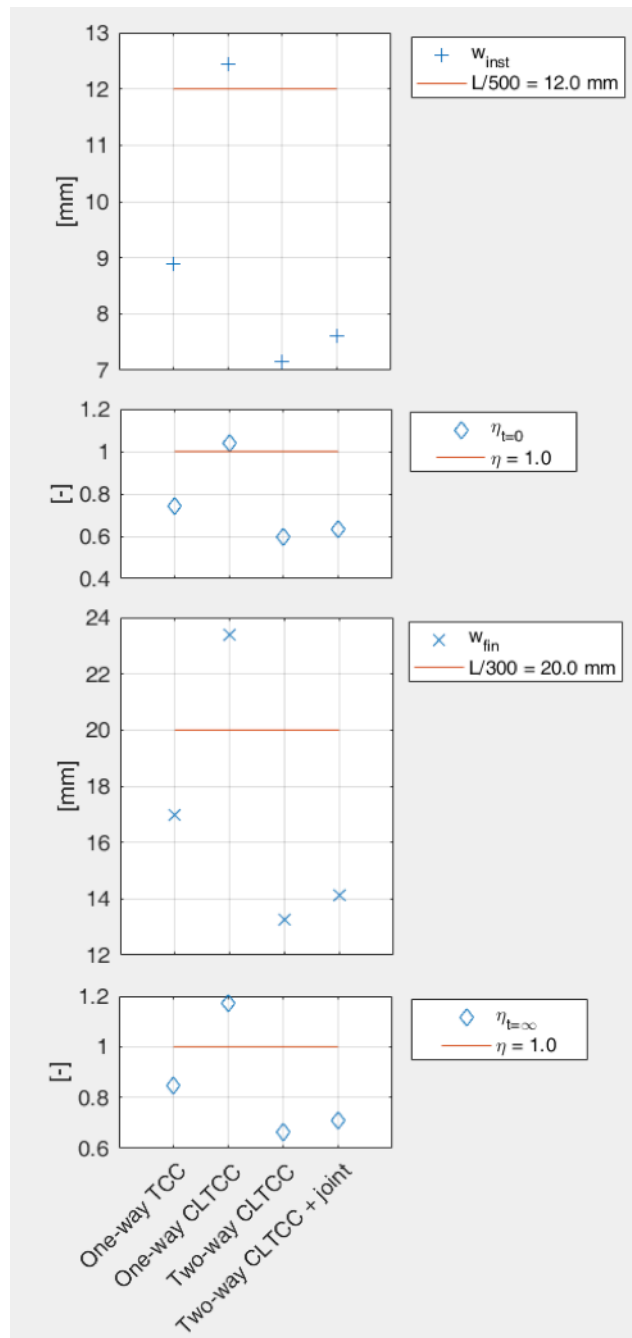


Figure 14: Comparison by deflection of different timber-concrete-composite slabs.

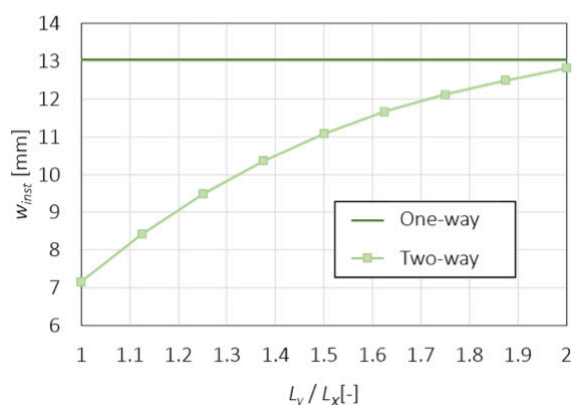


Figure 15: Influence of the side length ratio on the maximum deflection.

for the assembly two-way spanning CLTCC according to Section 4.6 and $L_x = 6.0$ m. The result is given in Figure 15. With a side length ratio $L_y / L_x = 2.0$ the deflection of the two-way spanning slab converges the one-way spanning.

5 CONCLUSION

The applicability of the TCC-construction method for two-way spanning systems was demonstrated. Solutions for the arrangement of shear connectors and CLT-layers within the slab were found. The influences of torsion on the plate load-bearing behaviour was determined. With glued-in reinforcement bars, a connection was developed, which meets the requirements of stiffness and practical buildability. A comparison with one-way spanning TCC-slabs shows distinct material reduction potentials.

The next step is to develop a calculation model for two-way spanning CLT-concrete-composites that can be applied with established instruments in practice.

6 REFERENCES

ANSYS 17.1 (2016): Finite-element-software. Workbench, Release 17.1, Ansys Inc.

Blaß, H. J. et al. (1995): Trag- und Verformungsverhalten von Holz-Beton-Verbundkonstruktionen. Research report. Karlsruhe Institute of Technology.

Blaß, H. J. et al. (2006): Tragfähigkeit von Verbindungen mit selbstbohrenden Holzschrauben mit Vollgewinde: Karlsruher Berichte zum Ingenieurholzbau 4. Karlsruhe Institute of Technology.

DIN EN 1991-1-1/NA (2010): National Annex - Nationally determined parameters - Eurocode 1: Actions on

structures - Part 1-1: General actions - Densities, self-weight, imposed loads for buildings. DIN.

DIN EN 1995-1-1/NA (2013): National Annex - Nationally determined parameters - Eurocode 5: Design of timber structures - Part 1-1: General - Common rules and rules for buildings. DIN.

EN 338 (2016): Structural timber - Strength classes. CEN. Brussels

EN 1991-1-1 (2010):

Eurocode 1: Actions on structures - Part 1-1: General actions - Densities, self-weight, imposed loads for buildings. CEN. Brussels

EN 1992-1-1 (2011): Eurocode 2: Design of concrete structures - Part 1-1: General rules and rules for buildings. CEN. Brussels.

EN 1995-1-1 (2010): Eurocode 5: Design of timber structures - Part 1-1: General - Common rules and rules for buildings. CEN. Brussels.

EN 16351 (2015): Timber structures - Cross-laminated timber - Requirements. CEN. Brussels.

EN 26891 (1991): Timber structures; joints made with mechanical fasteners; general principles for the determination of strength and deformation characteristics. CEN. Brussels.

ETA-13/0029: Wuerth ASSY Plus VG: Self-tapping screws for use in wood-concrete slab kits. Valid from 01/2013 to 07/2017. ETA Denmark.

ETA-09/0036: MM-crosslam: Solid wood slab elements to be used as structural elements in buildings. Valid from 06/2013 to 06/2018.

Kudla, K. (2015): Notched Connections for TCC Structures as Part of the Standard: COST Action FP1402 - Short Term Scientific Mission. Report. University of Stuttgart.

Leonhardt, F. et al. (1973): versuche zur Ermittlung der Tragfähigkeit von Zugschlaufenstößen. In: Deutscher Ausschuss für Stahlbeton, Band 226.

Loebus, S. and Winter, S. (2017): Zweiachsige Tragwirkung bei Holz-Beton-Verbundkonstruktionen. Final report. Technical University of Munich.

Mestek, P. (2011): Punktgestützte Flächentragwerke aus Brettsperrholz (BSP) - Schubbemessung unter Berücksichtigung von Schubverstärkungen. Dissertation. Technical University of Munich.

Mestek, P. et al. (2011): TEILPROJEKT 15: TP 15 Flächen aus Brettstapeln, Brettsperrholz und Verbundkonstruktionen. Research report. Technical University of Munich.

Michelfelder, B. C. (2006): Trag- und Verformungsverhalten von Kernen bei Brettstapel-Beton-Verbunddecken. Dissertation. University of Stuttgart.

Steiger, R. (2012): In Brettschichtholz eingeklebte Gewindestangen: Stand des Wissens zu einer

leistungsfähigen Verbindungstechnik. In: Tagungsband 18. Internationales Holzbau-Forum.

Z-9.1-648: Würth ASSYplus VG Schrauben als Verbindungsmittel für Holz-Beton-Verbundkonstruktionen. Valid from 11/2012 to 11/2017. DiBt.

Z-9.1-705: 2K-EP Klebstoff WEVO-Spezialharz EP 32 S mit WEVO-Härter B 22 TS zum Einkleben von Stahlstäben in Holzbaustoffe, WEVO Chemie GmbH.